Author/s:
Canda, E;San Nicolas, R;Rupasinghe, M;Rasekh, H;Castel, A

Title:
Investigating Australian Calcined Clays as Supplementary Cementitious Materials

Date:
2025

Citation:
Canda, E., San Nicolas, R., Rupasinghe, M., Rasekh, H. & Castel, A. (2025). Investigating Australian Calcined Clays as Supplementary Cementitious Materials. Ceramics, 8 (1), https://doi.org/10.3390/ceramics8010009.

Persistent Link:
https://hdl.handle.net/11343/363261

ceramics

MDPI

Article

Investigating Australian Calcined Clays as Supplementary Cementitious Materials

Emily Canda [1], Rackel San Nicolas [2], Madhuwanthi Rupasinghe [2], Haleh Rasekh [1] and Arnaud Castel [1,*]

[1] School of Civil and Environmental Engineering, University of Technology Sydney (UTS), Sydney, NSW 2007, Australia; emily.r.canda@student.uts.edu.au (E.C.); haleh.rasekh@uts.edu.au (H.R.)
[2] Department of Infrastructure Engineering, University of Melbourne (UoM), Melbourne, VIC 3010, Australia; rackel.san@unimelb.edu.au (R.S.N.); madhuwanthi.rupasinghearach@unimelb.edu.au (M.R.)
* Correspondence: arnaud.castel@student.uts.edu.au

Abstract: Limestone Calcined Clay Cement (LC^3) has become a highlighted research topic over the past decade. Through various research, LC^3 demonstrated the capability to supplement portions of cement, highlighting the possibility to decrease CO_2 emissions due to the low calcination temperatures and low levels of CO_2 released from the material during calcination. At this stage, there is no research into the feasibility of LC^3 in any parts of Australia, limited research in finding clay, and incomplete research understanding how low calcination temperatures affect the compressive strength. The results show the feasibility of LC^3, where we demonstrated the feasibility of a low calcination temperature of 650 °C and found that various overburden waste clays (clay in quarries and mines that are not needed) across the East Coast of Australia produced comparable compressive strength results to conventional Portland cement-based mixes. The results also indicate that optimising the particle size distribution of the calcined clay enhanced both the workability and compressive strength of the mortars.

Keywords: low-grade clays; low calcination temperature; amorphous content; particle size; concrete strength; workability

Academic Editor: Mohamed Hamidouche

Received: 6 November 2024
Revised: 18 December 2024
Accepted: 31 December 2024
Published: 20 January 2025

Citation: Canda, E.; San Nicolas, R.; Rupasinghe, M.; Rasekh, H.; Castel, A. Investigating Australian Calcined Clays as Supplementary Cementitious Materials. *Ceramics* **2025**, *8*, 9. https://doi.org/10.3390/ceramics8010009

1. Introduction

Concrete is the most used construction material worldwide [1]. This is due to concrete being inexpensive compared with other materials and easily workable onsite [2]. The production of concrete makes up to 8% of the world's total emissions globally; however, the majority of these emissions are produced during the process of calcining limestone to manufacture cement [3]. Various supplementary cementitious materials have been heavily researched and are currently being used consistently in the Australian materials market. These materials include fly ash, which is a by-product of coal-fired power plants, and ground granulated blast furnace slag (GGBFS), a by-product from the blast furnace process [4,5]. It was predicted that there will be a decrease in fly ash availability in the future [6,7]. This can be attributed to the transition from coal-based manufacturing processes to alternative fuels. As the manufacturing industry adopts more sustainable energy methods, there will be a decline in the availability of fly ash and slag as raw materials. Another obstacle to using fly ash and slag as SCMs is their accessibility across different geographical locations. Some countries can access SCMs, as they have high manufacturing facilities. Meanwhile, countries that do not have access to industrial by-product-based SCMs have no alternative methods of producing sustainable concrete [8]. A future alternative to fly ash could be biomass ash [9], particularly because it addresses the

need for using locally available raw materials. However, Limestone Calcined Clay Cement (LC3) has become a highlighted research topic over the past decade.

The calcination of clay and the dehydroxylation of kaolinite are well understood [9–11]. However, there is still limited research on the low calcination temperatures of calcined clay and the effects on mortar compressive strength. Using a lower calcination temperature not only reduces both the energy consumption and embodied carbon but can also enable alternative methods of heating, allowing for the accessibility of creating the material worldwide.

Researchers have been collaborating with the industry to investigate clays and assess their suitability for LC^3 after calcination [12]. The locations where the clays were sourced are usually not provided [13,14]. In the case study by Akindahunsi et al. [15], the location where the clay was sourced from was disclosed, providing confidence in obtaining feasible clay for LC^3. However, there is still limited research into the process of choosing sites for economic benefit. This aspect was included in this study to address the critical thought process behind discovering possible sites that signify kaolinite availability. The effect of the calcined clay particle sizing was also investigated in this study. Zunino et al. [16] observed a higher strength at early ages when utilising both coarse and fine limestone and presented an opportunity to understand the effects of the particle sizing and surface area of the calcined clay on the mechanical properties of mortar. Additionally, research conducted by Navarrete et al. [17] and Maier et al. [18] provided valuable insights into the intricate role of calcined clay properties in influencing concrete properties. The results suggest a direct correlation between a denser matrix and enhanced concrete strength.

The opportunity to discover viable clays on the East Coast of Australia exists. The research aims to significantly reduce CO_2 through finding waste clays near manufacturing facilities (to reduce transportation) and exploring the possibility of using low calcination temperatures. In this study, waste clay refers to material that is not utilised by quarries or mines because operations prioritise other resources, leaving the clay located between layering sheets, unsuitable for use.

This research investigated the viability of LC^3 by utilising overburden waste quarry/mining material from the East Coast of Australia. This research investigated the minimal calcination temperature of 650 °C to prioritise sustainability, whilst also researching various particle sizes of the calcined clay and their effects on both the flow and compressive strengths of mortars, meaning better mix designs, water efficiency, and overburden material utilisation, as well as decreased CO_2 emissions. The opportunity to control the LC^3 concrete properties through designing the particle size of the calcined clay could revolutionise how mix designs are created today.

2. Materials and Methods

2.1. Preselection of Suitable Sites with Overburden Clay Material

A main goal of this research was to identify sites with more than 3 million tonnes of overburden material that are located less than a distance of 80 km from an existing kiln along the East Coast of Australia. After selecting the particular sites, the clay was tested for kaolinite content, and the sites that consisted of clay with a kaolinite content greater than 25% were selected for further analysis. Overburden clay from 9 sites were initially investigated, and clay from only four sites (named as Site A, Site B, Site C, and Site D) satisfied these requirements. All samples were collected above ground, as this research project was targeted to utilise overburden material. Sampling followed procedures as recommended by Snellings, Almenares Reyes [19], with the addition of isolating a 1 m^2 section and taking a representative sample. Samples were collected in large quantities of 1–5 kg in plastic bags and labelled accordingly with the coordinates of the location.

2.2. Methods Adopted for the Characterisation of Raw Clays

All clay samples were dried in an oven for 7 days at 100 °C to help dry out the clay in preparation for kaolinite content determination, as specified by Avet and Scrivener [20]. This method utilised a furnace. Once dried, the samples were crushed with a mortar and pestle, then sieved to obtain material passing through a 4mm sieve. Three heating steps at 200 °C, 400 °C, and 600 °C were used. The data at 400 °C and 600 °C were used to determine the kaolinite content, and the data at 200 °C were used for calculations of the moisture state of the clay. This methodology was chosen due to the straightforwardness of the procedure. The equation stated below calculates the mass lost during the kaolinite dehydroxylation, leading to the determination of the kaolinite content:

$$wt\%_{kaolinite} = wt\%_{kaol-OH} \frac{M_{kaolinite}}{2\, M_{water}} \quad (1)$$

where $wt\%_{kaol-OH}$ is the mass lost due to the dehydroxylation of kaolinite, $M_{kaolinite}$ is the molecular weight of kaolinite, and M_{Water} is the molecular weight of water. The constant 2 corresponds to 2 moles of water being chemically bound to one mole of kaolinite [21].

Clay from the selected sites was prepared to undergo further analysis of X-ray diffraction (XRD), Thermal Gravimetric Analysis (TGA), and X-ray fluorescence (XRF). For all these investigations, the material was dried out similarly as mentioned above, then milled through an Essa ring mill for 30 s. A Bruker D8 Discover X-ray diffractometer was utilised for the XRD. The diffractometer operated in a continuous configuration, where it utilised copper as the source material with a fixed slit size of 0.5°. The investigated angular range was between 5 and 70 [°2θ], with a step size of 0.026°2θ. External Rietveld analysis was carried out using anatase as the external reference sample. The analysis was conducted via Highscore 4.5 and Profex 4.3.4 software, which were used to characterise the mineralogy of each selected clay.

For the selected clays, TGAs were performed using Mettler-Toledo TGA/DSC 2 equipment, with a temperature range of 50–1150 °C. A heating rate of 10 °C per minute was used, along with a nitrogen gas flow rate of 50mL/min to confirm the kaolinite content and understand the dehydroxylation of each specific clay, which also helped determine the suitable calcination temperature. The oxide compositions of raw clay were obtained by wavelength-dispersive X-ray fluorescence (WD-XRF) using the PANalytical AXIOS instrument.

2.3. Methods Adopted for the Characterisation of Calcined Clays

The Standard Test Method for Measuring the Reactivity of Supplementary Cementitious Materials by Isothermal Calorimetry and Bound Water Measurement C1897–20 ASTM [22] was conducted to understand the differing reactivities based on the calcination temperatures on sample BCC at 650 °C, 700 °C, 750 °C, and 800 °C, where all temperature durations were 45 min (Appendix A). Methodology A: Cumulative Heat Determination by Isothermal Calorimetry was used. After experimentation through standard C1897-20 [22], 650 °C at 45 min was selected as the calcination temperature of all the selected clay samples. As the difference in terms of reactivity between the different calcination temperatures were not significantly different, 650 °C was chosen for further testing to understand the results from using a low calcination temperature and a short time. It was then confirmed through the XRD of the selected clay material that the kaolinite demonstrated minimal kaolinite peaks after being calcined at 650 °C for 45 min. This established a baseline calcination procedure and secured a consistent methodology.

The characterisation via TGA of all the calcined clays confirmed that the main dehydroxylation occurred after 400 °C, with minimal water loss observed beyond this point, indicating the completion of calcination, as further discussed later. Characterisation via the XRD of the selected calcined clays confirmed the amorphisation, thus confirming the trans-

formation into metakaolin. The XRD was also used to determine the phase compositions through external standard Rietveld analysis, using anatase as a reference.

After calcining all the clays, the optimal milling time was established by milling 100 g of each clay using the Essa Steel ring mill. The particle size distribution was observed using a Malvern Mastersizer 3000 with the sample dispersed in water. The optimal milling time was necessary to understand, as at a certain time point, each clay would agglomerate at different milling durations. The four Australian calcined clays (ACC, BCC, CCC, and DCC) from Sites A, Site B, Site C, and Site D, respectively, were all milled for 10, 20, 30, and 40 s with 100 g of each material. It was obvious that each material began to agglomerate at a certain time, as instead of the size decreasing with the increase in milling time, it would begin to increase. The time before the sudden increase was selected for each clay, as this indicated the least agglomeration.

To understand the effects of the particle sizing of the calcined clay, 300 g of calcined clay was also milled and sieved to less than/passing 45 µm in preparation for the mortar to determine the effects of the particle size and surface area on the mortar flow. The Brunauer, Emmett, and Teller (BET) surface areas of the clays, both in raw and calcined form, were analysed via IQsorb Nitrogen Absorption, where pre-soak degassing occurred at 60 °C for 45 min, then at 270 °C for 3 h to ensure any impurities would not harm the experiment.

2.4. Materials and Mix Design

General Purpose (GP) cement in compliance with AS 3972, commercial fly ash, and fine limestone (supplied by Omya Australia and containing more than 95 wt% $CaCO_3$) were used as the cementitious material in all mixes. The selected clay material from sites A, B, C, and D (denoted as ACC, BCC, CCC, and DCC, respectively) were investigated as calcined clay. Two commercially available calcined clay materials from India (ICC) and France (FCC) were also investigated as reference materials for comparison purposes. The sand used in the mortar mixes was Normensand, which is in line with EN 196-1 [23].

All of the Australian clays were characterised both in their raw form and calcined form before the experimentation. The details of the methodology of characterisation are outlined in Sections 2.2 and 2.3. The particle size distributions (PSDs) of all the calcined clays prepared to pass 45 µm and at their optimal milling times are summarised in Table 1. Two of the commercial calcined clays (ICC and FCC) were readily available and had been used in previous studies [24,25]. ICC and FCC are both considered reference clays, which were analysed via a Rietveld analysis (external method) to determine the amorphous content as a substitution for understanding the kaolinite content, as these reference samples came calcined.

Table 1. Particle size distributions of clay (i) sieved through 45 µm and (ii) subjected to optimal milling times.

Calcined Clay Name	Calcined Clay Sieved to 45 µm Characterisation				Calcined Clay at Optimal Milling Times			
	PSD (%)			BET Surface Area (m^2/g)	PSD (%)			BET Surface Area (m^2/g)
	10 v (10% Passing the Below Micron (µm)	50 v (50% Passing the Below Micron (µm)	90 v (90% Passing the Below Micron (µm)		10 v (10% Passing the Below Micron (µm)	50 v (50% Passing the Below Micron (µm)	90 v (90% Passing the Below Micron (µm)	
ICC	2.90	17.4	51.2	7.4	3.8	14.4	43.3	8.8
FCC	2.50	14.7	38.7	14.0	2.5	21.1	64.7	12.5
ACC	2.30	12.1	69.7	15.5	2.7	14.5	86.4	11.4
BCC	0.04	9.5	68.0	43.7	3.5	31.1	111.0	31.8
CCC	2.00	10.5	38.2	17.4	2.6	12.7	51.8	15.8
DCC	2.20	15.0	56.0	29.4	3.3	28.3	112.0	33.7

The mortar experimentation was performed as per ASTM C109 [26]. The details of the mix design are stated in Table 2. The GP reference mix with 100% GP (denoted as GP-R) and fly ash reference mix with 70% GP and 30% FA (denoted as FA-R) were designed as baselines for all the mixes under investigation.

Table 2. Mortar mix design for the 14 different mixes (w/b ratio 0.44).

Calcined Clay Used	Mix Name (Using 45 µm Clay)	Mix Name (Using Optimised PSD)	GP (g)	FA (g)	Limestone (g)	Calcined Clay (g)	Sand (g)
-	GP–R	-	450	-	-	-	1350
-	FA–R	-	315	135	-	-	1350
Commercial metakaolin (from India)	ICC	ICC–O	315	-	45	90	1350
Commercial metakaolin (from France)	FCC	FCC–O	315	-	45	90	1350
Site A	ACC	ACC–O	315	-	45	90	1350
Site B	BCC	BCC–O	315	-	45	90	1350
Site C	CCC	CCC–O	315	-	45	90	1350
Site D	DCC	DCC–O	315	-	45	90	1350

Six mixes with calcined clay sieved through a 45 µm sieve (2 references and 4 Australian clays), including 70% GP, 20% calcined clay, and 10% limestone, were included in this study. Additionally, six optimal PSD calcined clay mixes (2 references and 4 Australian clays), including 70% GP, 20% calcined clay, and 10% limestone, were designed and prepared.

The w/b ratio for the mortar mixes was 0.44 according to ASTM C109 [26], which achieved a flow of 106 cm. No gypsum was added into any of the mixes due to the GP cement having up to 7.5% gypsum and the fact that the 30% replacement rate of cement is considered a low replacement. The flow for each mix was measured using a flow table according to ASTM C1437-20 [27].

Mortar was mixed according to ASTM C305-20 [28] using a mortar mixer with low and high speeds of 140 rpm and 285 rpm, respectively. Mortar samples were tested at 1 day, 3 days, 7 days, 28 days, and 90 days, as per ASTM C348-21 [29] and ASTM C-1698 [20]. Two specimens were tested at each maturity, and the average values are reported. In addition, pastes (with no sand) were also created for isothermal calorimetry using the 45 µm calcined clays.

3. Results and Discussion

3.1. Exploration of Clays and Characterisation

All the samples' appearances and textures were vastly different from each other, as indicated in Figure 1. The material textures ranged from sandy, rocky, clayey, and rubble, with all the materials found indicating various levels of kaolinite content.

The overburden clay samples from nine different sites located along the East Coast of Australia were initially investigated based on the EPFL tangent method [30] for quick determination of the kaolinite content. Out of the nine sites, four sites were determined to continue with the further analyses and characterisations of the properties. The selection was based on the sites that demonstrated kaolinite contents greater than 25%. Figure 2 summarises the kaolinite contents of the various sites investigated. The kaolinite contents initially obtained through the EPFL tangent method were also verified through the XRD and TGA methods. It can be observed that the clays from sites A and B had similar kaolinite contents (around 44%).

The clays from sites C and D had kaolinite contents around 35%. The clays from sites E, F, G, H, and I were not further investigated due to their low kaolinite contents.

Figure 1. The various clays drying in the oven.

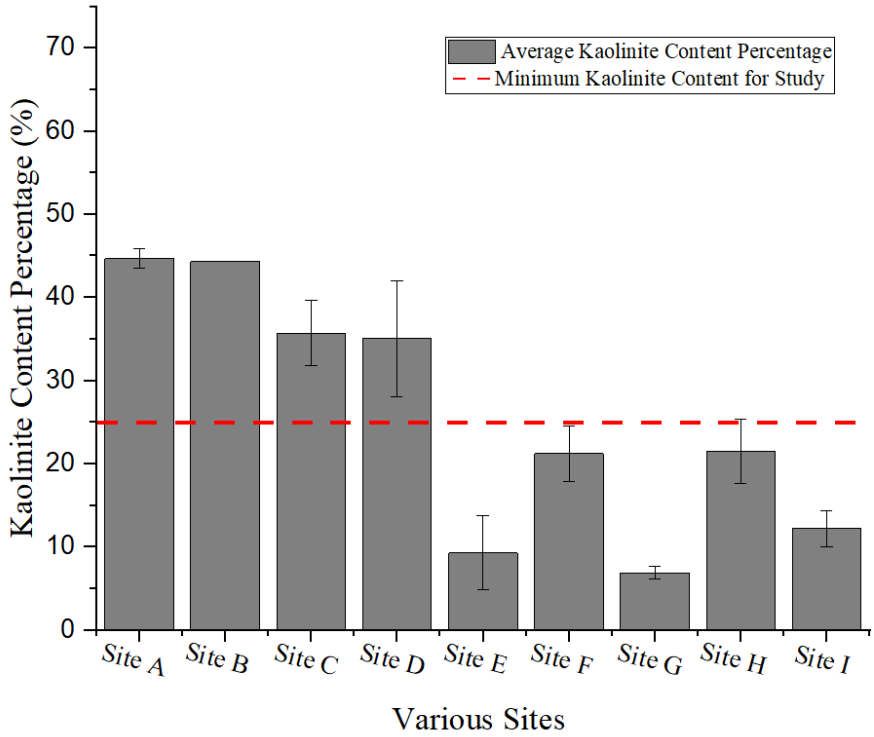

Figure 2. The kaolinite contents of the samples collected per site were determined via the EPFL tangent method.

The crystalline phases present in the raw clays for the four selected sites are shown in Figure 3a. All clays indicated kaolinite contents with peaks visible at 12–13° 2θ. ARC and CRC indicated high levels of quartz, whilst BRC and DRC indicated low levels of quartz. The XRD results confirm the presence of high kaolinite contents in the selected clay samples. This proved the feasibility of further testing and experimenting with the selected clay samples based on the EPFL tangent method.

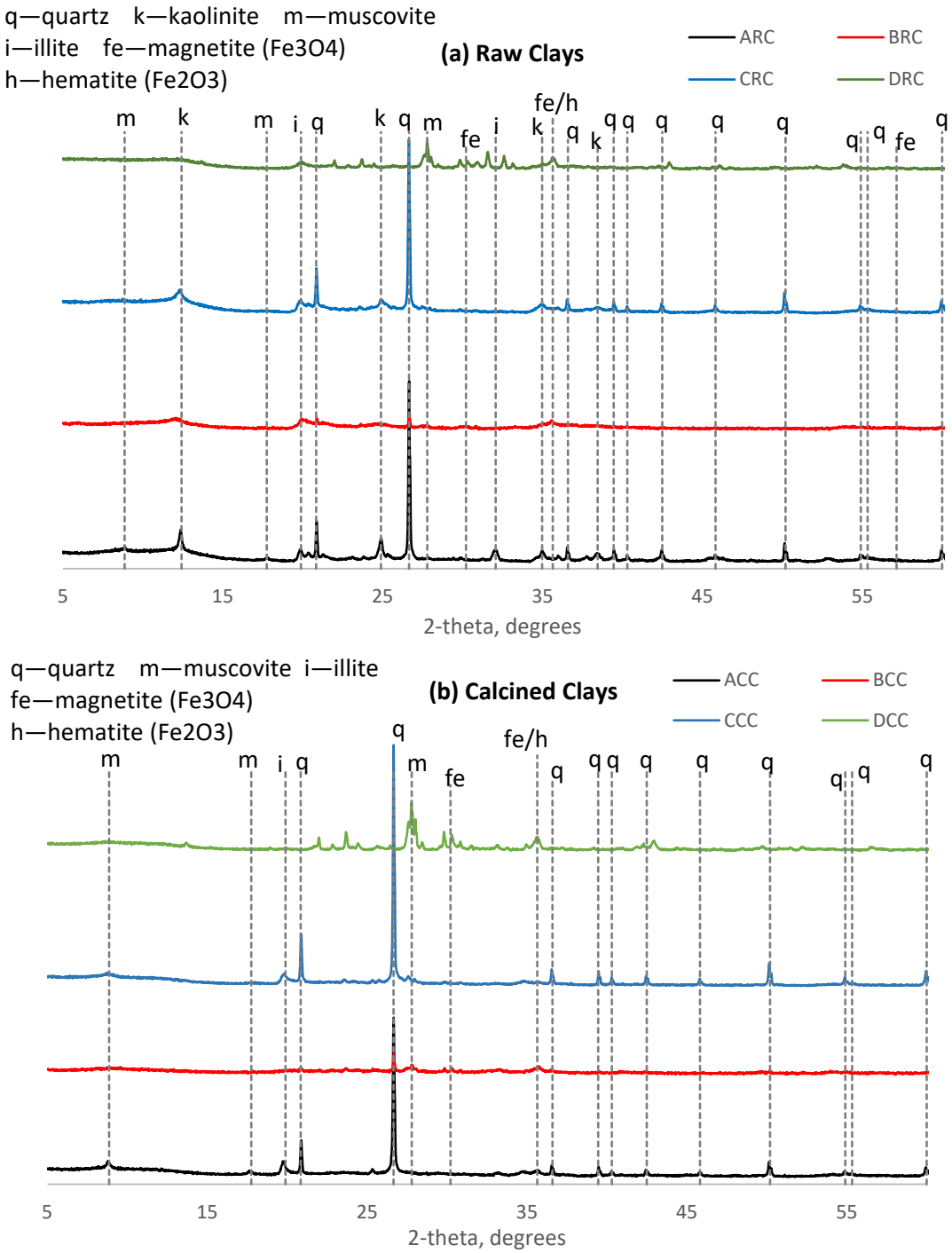

Figure 3. Phases present in the (**a**) Australian clay (raw clay) from the XRD analysis and (**b**) Australian calcined clays from the XRD analysis.

X-ray diffraction was conducted on all the Australian calcined clays (ACC, BCC, CCC, and DCC) and the diffraction patterns are denoted in Figure 3b. The XRD of the calcined clays confirmed the successful transformation of kaolinite to metakaolin, as the kaolinitic peaks were no longer visible. The XRD data correlated well with the XRF data and colours of the different clays. The two clays BCC and DCC exhibited a red colour due to the presence of iron-containing minerals, which was also confirmed by the XRF analysis. Most of the clays contained high quartz, referring to Si; however, BCC showed the lowest quartz amount and Si amount according to the XRF. As the XRD results show, all of the clays were mixed with various minerals, as expected for any overburden clay material.

The external Rietveld analysis method via XRD confirmed a high amorphous content in most of the calcined clays (Table 3). Clays ACC and BCC had the highest kaolinite contents (44%). However, ACC indicated the lowest amorphous phase content (46.1%) and BCC indicated the highest amorphous content (66.5%) out of all the Australian calcined clays. The XRD investigations (Figure 3b and Table 3) for BCC indicated iron compositions (which was also confirmed through the XRF, as described later on). BCC had the lowest quartz content compared with all the other Australian clays. Clay CCC indicated mostly quartz, which linked directly to the high Si indicated in the XRF results (Table 4). Clay DCC also revealed varying phases with higher amounts of Si and Fe, which linked to its strong red colour.

Table 3. Simplified phases present in the calcined clays were analysed via the XRD.

Phases	ICC	FCC	ACC	BCC	CCC	DCC
Amorphous (%)	73.4	56.2	46.1	66.5	65.3	53.5
Anatase (%)	2.0	-	-	-	-	-
Hematite (%)	2.3	0.4	-	1.2	-	-
Mullite (%)	1.0	2.1	-	-		-
Quartz (%)	15.2	20.3	17.1	2.6	24.7	14.2
Illite (%)	-	-	8.3	-	4.4	-
Muscovite (%)	-	-	-	-	9.3	-

Table 4. Oxide compositions analysed via XRF of calcined clays.

Sample	CaO	SiO_2	Al_2O_3	Fe_2O_3	SO_3	MgO	K_2O	TiO_2	Na_2O	P_2O_5	Mn_2O_3	LOI	Total + LOI	Moisture
ICC	0.14	48.4	41.75	2.25	0.11	0.05	0.05	3.38	0.23	0.08	0.01	3.33	99.78	0.35
FCC	0.49	74.5	19.28	2.04	0.03	0.11	0.17	0.95	0.03	0.04	0.01	2.17	99.82	0.54
ACC	1.08	58.08	23.01	9.27	0.17	1.4	2.59	0.89	0.07	0.48	0.18	2.58	99.8	0.64
BCC	2.4	42.22	23.88	18.73	0.04	3.43	0.52	2.71	0.76	0.28	0.2	4.94	100.11	1.45
CCC	0.1	65.92	19.64	5.59	0.08	0.7	2.27	0.75	0.37	0.03	0.12	4.12	99.69	1.36
DCC	4.94	56.46	14.23	9.69	0.07	3.4	1.19	1.44	1.16	0.12	0.11	6.99	99.8	1.79

The reference clays, due to already being calcined before arriving, were not investigated for their kaolinite contents. Therefore, only the amorphous phase was discovered through this testing.

Thermogravimetric analysis of the clays confirmed the kaolinite content of each clay. The results of the kaolinite content estimated via Figure 4a are similar to the kaolinite content estimation via the EPFL tangent method, only differing within 5%. The dehydroxylation point was also confirmed for all the Australian clays as being between 450 °C and 600 °C, with the complete dehydroxylation of kaolinite at 600 °C. Thermogravimetric analysis (TGA) was completed post-calcination to determine the complete dehydroxylation. The first mass loss of the uncalcined clays in Figure 5a was observed around 100–150 °C, which was linked to the evaporation of the physically absorbed water on the external surfaces of the kaolinite [30]. Dihydroxylation (removal of OH groups) in clay minerals causes a peak in the range of 400–800 °C. The position of this peak depends on the type and structure of the clay minerals, as well as the binding of hydroxyls. Kaolinite dihydroxylation occurs between 400 and 600 °C [9]. With comparatively high kaolinite contents in the clays investigated, a second main peak occurred due to the dihydroxylation of kaolinite within the range of 400–600 °C, as depicted in Figure 4a. The peak that occurred between 200 and 350 °C in the DTG results for BRC and DRC was due to the decomposition of iron oxyhydroxides [31]. This agreed well with the XRD phase identification, where diffraction patterns for BRC and DRC confirmed the presence of iron-containing phases (Figure 3a). As demonstrated in Figure 5b, the calcined material only lost minimal mass related to the moisture loss of the calcined clays. Also, the kaolinite dehydroxylation peak

that occurred in the range of 400 °C to 600 °C significantly reduced for the calcined clays, which confirmed the successful transformation of kaolinite into metakaolin.

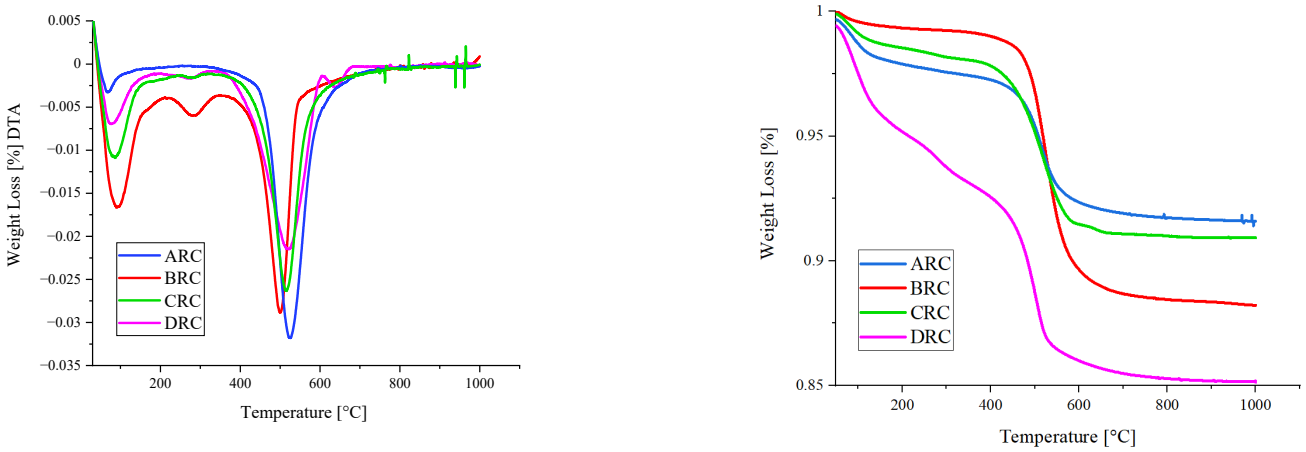

(**a**) (**b**)

Figure 4. (**a**) Differential weight loss of the Australian raw clays through thermogravimetric analysis; (**b**) thermogravimetric analysis results of the Australian raw clays (ARC, BRC, CCC, DRC).

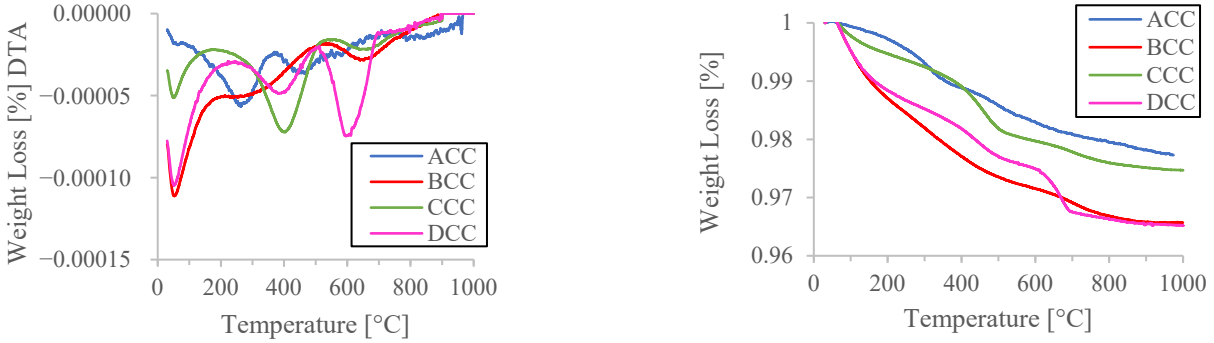

(**a**) (**b**)

Figure 5. (**a**) Differential weight loss of the Australian calcined clays through thermogravimetric analysis; (**b**) thermogravimetric analysis results of the Australian calcined clays (ACC, BCC, CCC, DCC).

The chemical compositions via X-ray fluorescence are represented in Table 4 and the normalised ternary graph displaying the chemical compositions is given in Figure 6. The reference clays FCC and ICC had the lowest and highest Al_2O_3 contents, respectively, out of all the investigated calcined clay materials. All calcined clays were within the natural pozzolan range, which demonstrated the feasibility of using them as cementitious material. As depicted, ACC and BCC demonstrated higher amounts of alumina compared with the other Australian clays. This can be correlated to the high kaolinite content that was present in the ARC and BRC samples.

Calcium oxide was measured as low in all the samples, while CCC demonstrated the highest silica content at 65.92% out of the Australian samples, followed by ACC at 58.08%. From all the samples, FCC (the reference sample) indicated the highest quantity of silica (74.5%). These XRF results were also consistent with the XRD quantification analysis, which confirmed the highest quartz content for CCC among all the Australian clays.

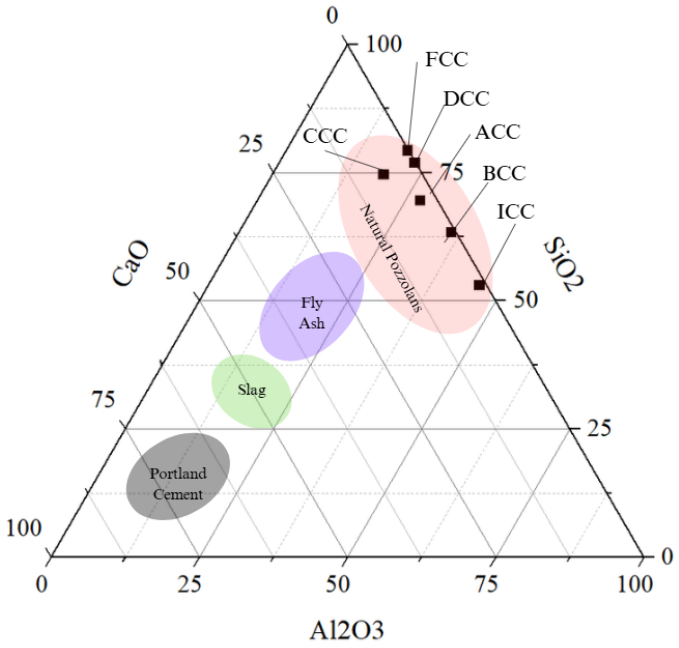

Figure 6. Normalised ternary diagram showing the different Australian calcined clay compositions, as well as common cementitious material regions adapted from Lothenbach [31].

3.2. Reactivity and Calorimetry of Pastes

The R3 test was conducted to evaluate the pozzolanic reactivity of the calcined clay material. The normalised calorimetry results are depicted in Figure 7. The results illustrate the feasibility of the local clay material calcined at 650 °C. All calcined clay material showed a higher heat released than the FA mix. However, all the calcined-clay-based pastes exhibited a lower heat release compared with that of the GP-based mix.

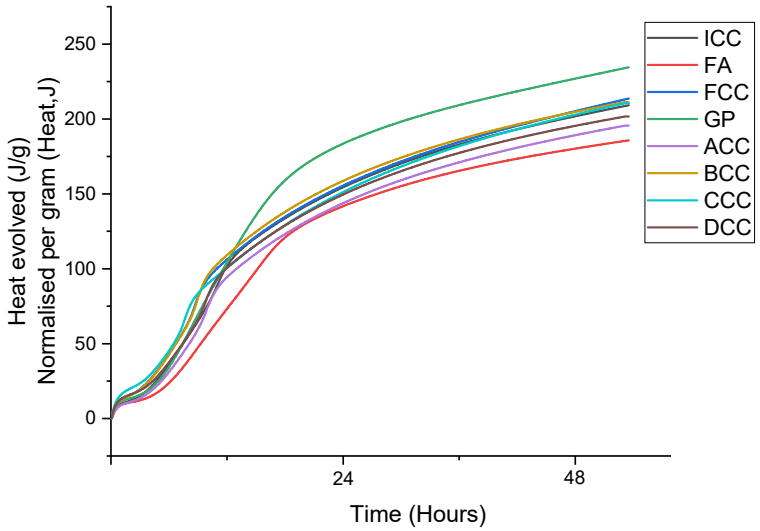

Figure 7. The heat released for the various calcined clay mixes with blends of 70% GP and 10% limestone.

The calorimetry results of the LC^3 paste (Figure 7) were in line with the amorphous content of each calcined clay. The reference GP mix indicated the highest heat released and the reference FA mix demonstrated the lowest heat. Even though ARC possessed the highest kaolinite content at 44.7%, upon calcination, it exhibited the lowest amorphous content of 46.1%. Notably, ACC released less heat compared with all the other Australian clays (BCC, CCC, and DCC), which had lower kaolinite and higher amorphous contents than ACC.

3.3. Mortar Results

3.3.1. Flow

Standard C1437–20 [27] was used to test and measure the hydraulic cement mortar flow using a flow table. All LC^3 mixes achieved flow that was much less than the reference mixes of GP and FA. No superplasticisers were used in this study with the aim of understanding the basic mechanical properties of each calcined clay mix in the application of mortars. The 45 µm calcined clay mortars achieved flow values lower than the calcined clay with optimised PSD (Figure 8). The calcined clays with the optimal PSD demonstrated better flow with the same design w/b ratio.

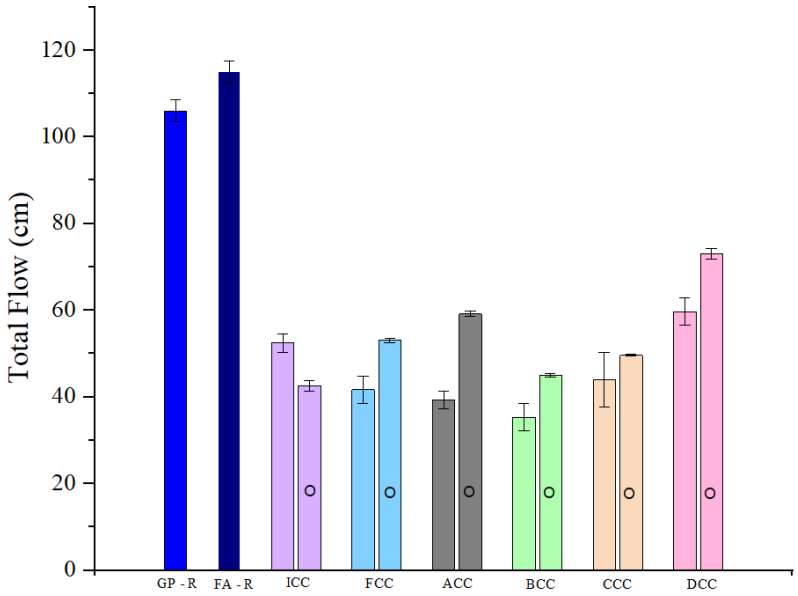

Figure 8. Flow of all mixes next to their respective optimised particle size flow (O).

Lorentz et al. [32], reported that high metakaolinite content determined the rheology properties, rather than the PSD. It was difficult to compare the results, as the experiments were not identical. However, the results presented in Figure 8 indicate that the PSD affected the flow of the mortars. The surface area characteristics did not change dramatically between the optimal PSD and 45 µm PSD, though the change to a larger PSD contributed to better workability of the mortar in the case of all the calcined clay mixes. Sample ICC depicted less flow with the optimised PSD, which correlated well, as the optimal PSD was smaller in the case of the optimised ICC compared with the 45 µm ICC. Further assessments on concrete would be necessary to establish this knowledge in practical applications.

3.3.2. Compressive Strength Results

Mortars were tested at 1, 3, 7, and 28 days according to ASTMC348-19 [29]. The PDS optimisation of the Australian calcined clays did not improve the compressive strengths of the mortars after one day. A marginal reduction in strength could be observed mostly for ACC and CCC mortars. Overall, the one day compressive strengths of all the LC3 mortars were consistent with the reference GP–R and superior to the fly ash mortar FA–R. From the third day of testing, all the Australian calcined clay mortars with the optimised calcined clay PSD achieved a significantly higher compressive strength (Figure 9b) than the counterpart 45 µm calcined clay mortars (Figure 9a). The coarser PDS of the optimised calcined clays improved both the workability (Figure 8) and compressive strength.

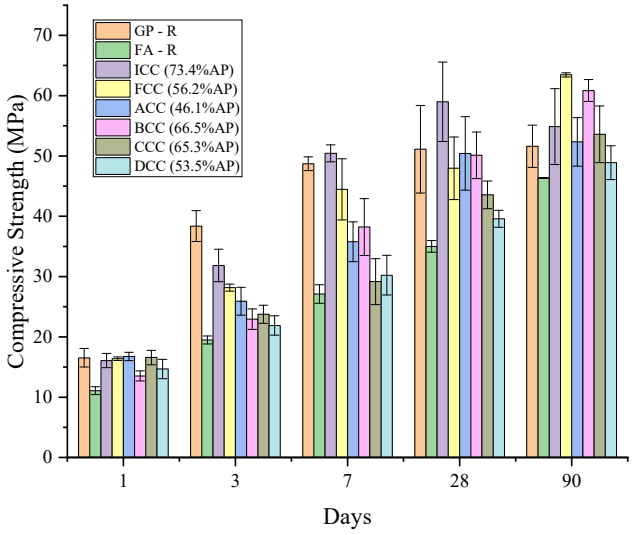

(**a**)

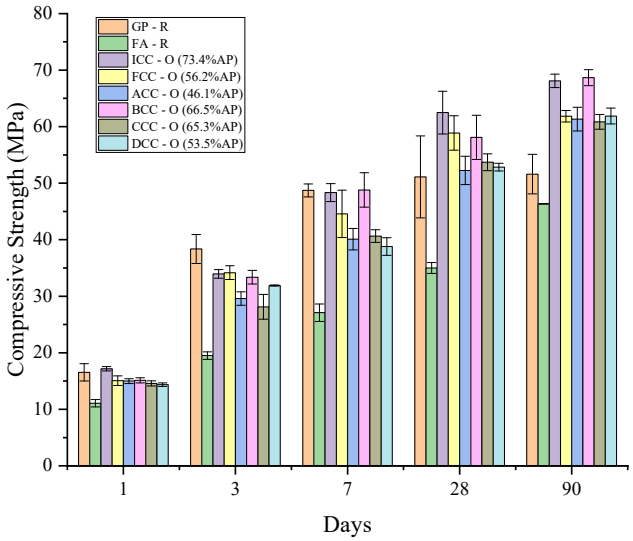

(**b**)

Figure 9. Compressive mortar strengths of all mixes, including LC^3 and reference mixes, using (**a**) calcined clay sieved to 45 μm for >LC^3 mixes and (**b**) optimally sized calcined clay for LC^3 mixes.

After 3 days, the reference GP–R compressive strength was superior to that of all the Australian calcined clay mortars with the optimised calcined clay PSD. The best-performing Australian calcined clay mortar was BCC, with only about a 15% strength reduction compared with GP–R, which was similar to the two other reference calcined clay mixes (ICC and FCC). The lowest-performing Australian calcined clay mortar was CCC, with about 25% strength reduction compared with GP–R. However, all the Australian calcined clay mortars outperformed the fly ash mortar FA–R.

After 7 days, BCC with the optimised calcined clay PSD achieved a similar compressive strength to the reference GP–R. The ACC, CCC, and DCC compressive strengths remained about 20% lower than that of GP–R. Studies showed that calcined clay with more than 40% kaolinite content can achieve similar/greater strengths than OPC at 7 days [33]; however, the present study did not show such results for the ACC, CCC, and DCC mortars. CCC and DCC's lower compressive strengths could be explained by the kaolinite content of the

clays being lower than 40% (Figure 2). The high quartz content in ACC might have been responsible for the lower 7 days compressive strength compared with BCC. But all the LC^3 mixes outperformed the FA–R reference at all ages, further demonstrating the feasibility of Australian limestone calcined clay as a supplementary cementitious material.

After 28 and 90 days, all the Australian calcined clay mortars with the optimised calcined clay PSD outperformed the reference GP–R, which could not be achieved by the 45 µm calcined clay mortars (Figure 9a). The optimal calcined clay sizing not only reduced the manufacturing time and embodied energy but also increased both the flow and strength. Furthermore, it was also revealed that the LC^3 mortar with BCC, which had a high kaolinite content and the highest amorphous content outperformed all Australian calcined clay mortars, leading to the highest compressive strength among samples with local clay material. This emphasises the importance of both the kaolinite content and the amorphous material content of calcined clay when using calcined clay as SCM. Whilst the lower-quality calcined clay mixes (ACC, CCC and DCC) did not achieve similar compressive strength as the reference mixes in the early ages, there are many suitable applications for these materials where the early age compressive strength of concrete is not that critical. Furthermore, this reduction in early age compressive strength is also observed in blended cement-based concretes using fly ash and/or GGBFS which are commonly used in practice.

Figure 10 depicts the correlation between mortar compressive strength, amorphous content, PSD and kaolinite content. It is understood that the time-dependent development of compressive strength is governed by each clay's characteristics, including mineralogy, chemistry and physical properties. For DCC, despite its low kaolinite content, the reasonable amorphous content and larger PSD resulted in a similar rate of strength development compared to the other clays (Figure 9b).

Figure 10 highlights the coefficient of determination (R^2) to help assess the correlations. The R^2 correlation in terms of the kaolinite content affecting the strength is very low with an R^2 value of 0.09 for 3 days and 0.15 for 28 days (Figure 10a,d). This does not agree with previous research reporting a high correlation between kaolinite content and compressive strength [9,16,34]. However, the narrow range of kaolinite content in the samples (35–44.7%) makes it more difficult to accurately depict a trend correlating kaolinite to strength. For further investigations, it is suggested to have a vast range of samples with larger differences in kaolinite content to accurately depict the correlation.

The particle sizing showed a high correlation at 3 days (Figure 10b), with an R^2 value of 0.80. This could have been due to particle packing occurring, which led to a higher strength at an early age. However, there was a low correlation between the particle size and the compressive strength at 28 days (Figure 10e), with a low R^2 value of 0.01.

The correlation between the amorphous content and the early age mortar strength at 3 days was low, with the R^2 value determined as 0.03. This could have been due to the slow reactivity of the calcined clays' amorphous phases, as seen in Figure 10c. Then, at 28 days (Figure 10f), a medium correlation between the amorphous phase and the mortar compressive strength was observed, with an R^2 factor of 0.57.

Figure 10 highlights the governing influence of the PSD on the early-age mortar compressive strength, with an added value of increased flow when utilising a more optimal particle size. Similar to the research from Zunino [16], having both fine and coarse gradings of calcined clay resulted in an improved performance compared with using only a fine particle sizing.

This study on different clays in relation to the mortar compressive strength further proved that the compressive strength of mortar was affected by a range of physical and chemical characteristics of calcined clay material and successfully confirmed the feasibility of low-kaolinitic clay types as potential SCMs. Low-kaolinitic clays, such as CCC and DCC,

should not be disregarded, as other characteristics can compensate for their low kaolinite content. As shown in Figure 9b, the 28-day compressive strength results for these clays was similar to that of ACC, which indicated the highest kaolinite content.

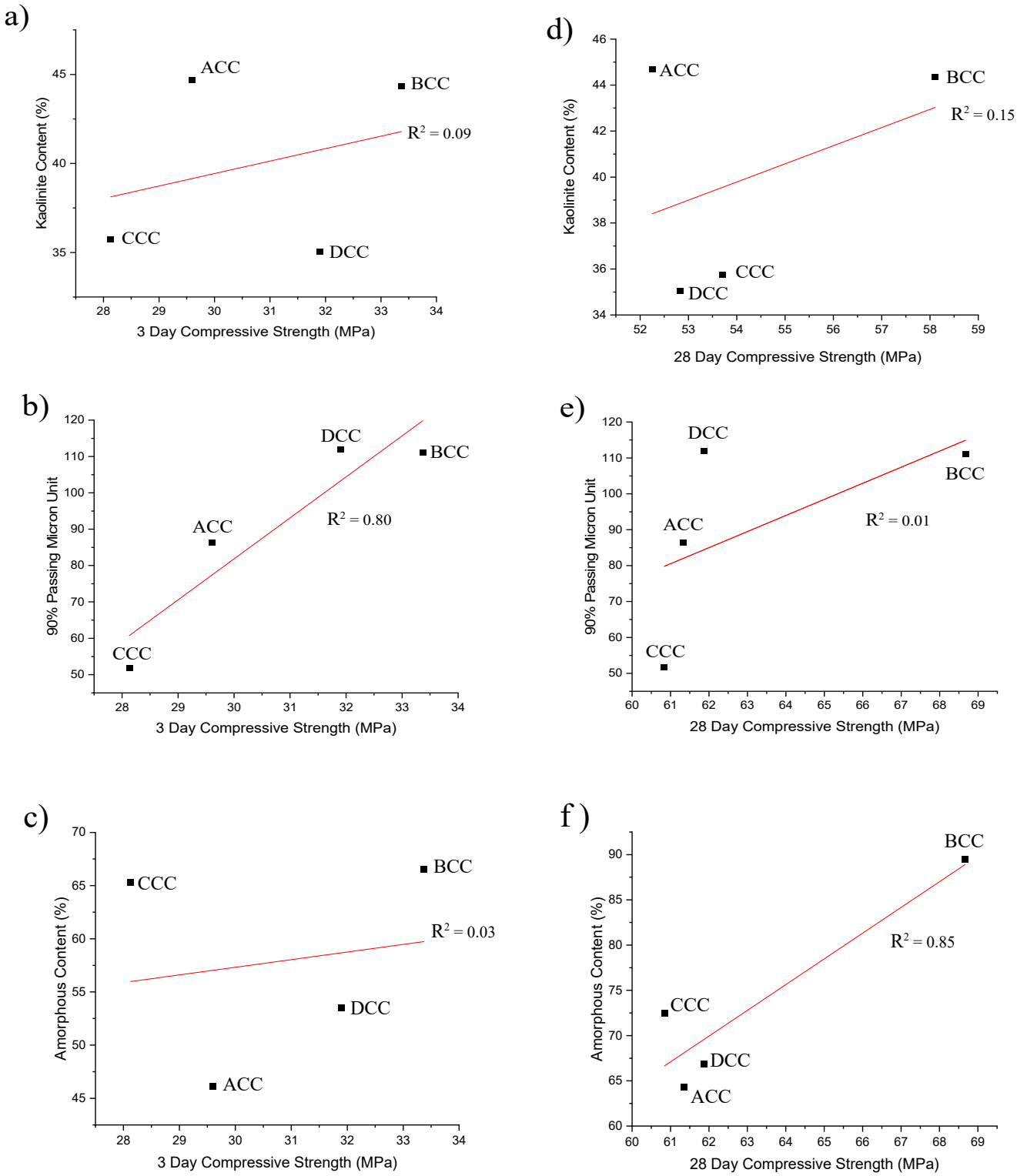

Figure 10. Relationships between the 3-day compressive strength and the (**a**) kaolinite content, (**b**) 90% passing PSD micron unit, and (**c**) amorphous content. Relationships between the 28-day compressive strength and the (**d**) kaolinite content, (**e**) 90% passing PSD micron unit, and (**f**) amorphous content.

4. Conclusions

This study aimed to assess the suitability of low-grade waste clays as SCMs following calcination and understanding the ability to calcine at a low temperature (650 °C). This study also aimed to investigate the influence of the calcined clay particle size distribution and its effects on both the flow and compressive strength in the application of mortar. Specific conclusions that could be drawn from this investigation are as follows:

- The optimisation of the particle sizing of the calcined clays, which involved transitioning to a larger PSD and smaller surface area, led to a higher LC^3 mortar compression strength in the early ages
- The calcination temperature of 650 °C at 45 min calcination time proved to be suitable for the Australian clays, where it calcined the kaolinite into metakaolin and demonstrated a suitable performance for potential calcined clay concrete applications.
- Low-kaolinitic clays should not be disregarded, as other characteristics can compensate for the low kaolinite content. As an example, a kaolinite content around 35% would be suitable if the PSD is optimised and the surface area ranges between 15 and 35 m^2/g after calcination.
- The Australian clays differed greatly between each other in terms of their characteristics. However, all the calcined clays in the application of LC^3 with the optimised PSD outperformed both references of GP-R and FA-R at 28 and 90 days in terms of the mortar compressive strength and outperformed FA-R at all ages. The PSD of the calcined clays should be considered as a major contributing factor when understanding compressive strength results.
- The LC^3 mortars were not as workable as the reference mixes. However, mortar mixes using calcined clays with an optimal PSD demonstrated improved flow characteristics while maintaining the same design water-to-binder ratio. Transitioning to a larger PSD and smaller surface area did contribute to a better mortar workability for all the calcined clay mixes, which can be improved further using superplasticisers.

Further research should be extended to determine the lowest possible temperature for calcining low-quality clays whilst also achieving comparable strengths to OPC. Research could also be further extended into understanding what calcined clay physio-properties can be manipulated to achieve a certain concrete or application result and also investigating the possibility of including higher ratios of calcined clay in concrete/mortar to further reduce OPC consumption.

Author Contributions: Methodology, E.C., A.C. and R.S.N.; Formal analysis, E.C., A.C., R.S.N., H.R. and M.R.; Writing—original draft, E.C., A.C., R.S.N., H.R. and M.R.; Supervision, A.C., R.S.N. and H.R.; funding acquisition, A.C. All authors have read and agreed to the published version of the manuscript.

Funding: This research was funded by the UTS—Boral Centre for Sustainability.

Institutional Review Board Statement: Not applicable.

Informed Consent Statement: Not applicable.

Data Availability Statement: The original contributions presented in the study are included in the article, further inquiries can be directed to the corresponding author.

Conflicts of Interest: The authors declare no conflict of interest.

Appendix A

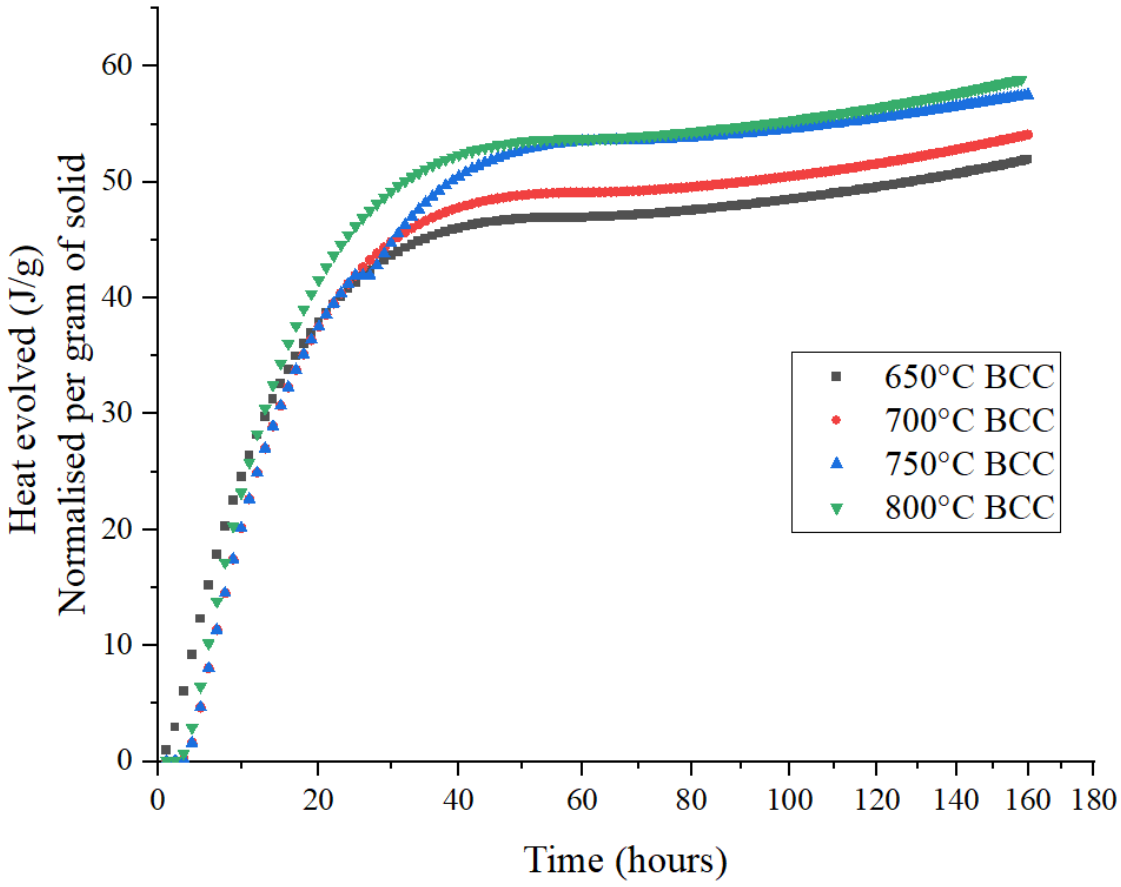

Figure A1. BCC heat released for calcination temperatures 650 °C, 700 °C, 750 °C, and 800 °C.

References

1. Lehne, J.; Preston, F. *Making Concrete Change Cement*; Chatham House: London, UK, 2018.
2. Gagg, C.R. Cement and concrete as an engineering material: An historic appraisal and case study analysis. *Eng. Fail. Anal.* **2014**, *40*, 114–140.
3. Bishnoi, S.; Maity, S. Limestone calcined clay cement: Opportunities and challenges. In Proceedings of the ICCCSC2019 Proceedings, Munich, Germany, 15–18 December 2019; p. 25.
4. Siddique, R.; Khan, M.I. Fly Ash. In *Supplementary Cementing Materials*; Springer: Berlin/Heidelberg, Germany, 2011; pp. 1–66.
5. Siddique, R.; Khan, M.I. Ground Granulated Blast Furnace Slag. In *Supplementary Cementing Materials*; Springer: Berlin/Heidelberg, Germany, 2011; pp. 121–173.
6. Change, C. Barriers to Net-Zero Concrete—Fly Ash and GGBS Shortage. 2022. Available online: https://www.concrete4change.com/post/barriers-to-net-zero-concrete-fly-ash-and-ggbs-shortage (accessed on 23 October 2022).
7. Malami, C.; Kaloidas, V.; Batis, G.; Kouloumbi, N. Carbonation and porosity of mortar specimens with pozzolanic and hydraulic cement admixtures. *Cem. Concr. Res.* **1994**, *24*, 1444–1454.
8. Díaz, Y.C.; Berriel, S.S.; Heierli, U.; Favier, A.R.; Machado IR, S.; Scrivener, K.L.; Hernández, J.F.M.; Habert, G. Limestone calcined clay cement as a low-carbon solution to meet expanding cement demand in emerging economies. *Dev. Eng.* **2017**, *2*, 82–91.
9. Frías, M.; de los Reyes, A.M.M.; Villar-Cociña, E.; García, R.; de la Villa, R.V.; Vasic, M.V. New Eco-Cements Made with Marabou Weed Biomass Ash. *Materials* **2024**, *17*, 5012. [CrossRef]
10. Fernandez, R.; Martirena, F.; Scrivener, K.L. The origin of the pozzolanic activity of calcined clay minerals: A comparison between kaolinite, illite and montmorillonite. *Cem. Concr. Res.* **2011**, *41*, 113–122.
11. Shvarzman, A.; Kovler, K.; Grader, G.; Shter, G. The effect of dehydroxylation/amorphization degree on pozzolanic activity of kaolinite. *Cem. Concr. Res.* **2003**, *33*, 405–416.
12. Nguyen, Q.D.; Khan, M.S.H.; Castel, A. Engineering Properties of Limestone Calcined Clay Concrete. *J. Adv. Concr. Technol.* **2018**, *16*, 343–357.

13. Tironi, A.; Scian, A.N.; Irassar, E.F. Blended Cements with Limestone Filler and Kaolinitic Calcined Clay: Filler and Pozzolanic Effects. *J. Mater. Civ. Eng.* **2017**, *29*, 04017116.
14. Avet, F.; Li, X.; Scrivener, K. Determination of the amount of reacted metakaolin in calcined clay blends. *Cem. Concr. Res.* **2018**, *106*, 40–48.
15. Akindahunsi, A.A.; Avet, F.; Scrivener, K. The Influence of some calcined clays from Nigeria as clinker substitute in cementitious systems. *Case Stud. Constr. Mater.* **2020**, *13*, e00443.
16. Zunino, F.; Scrivener, K.L. Influence of Kaolinite Content, Limestone Particle Size and Mixture Design on Early-Age Properties of Limestone Calcined Clay Cements (LC3). In Proceedings of the ICCCSC2019 Proceedings, Munich, Germany, 15–18 December 2019; Volume 2.
17. Navarrete, I.; Kurama, Y.; Escalona, N.; Lopez, M. Impact of physical and physicochemical properties of supplementary cementitious materials on structural build-up of cement-based pastes. *Cem. Concr. Res.* **2020**, *130*, 105994.
18. Maier, M.; Sposito, R.; Beuntner, N.; Thienel, K.-C. Particle characteristics of calcined clays and limestone and their impact on early hydration and sulfate demand of blended cement. *Cem. Concr. Res.* **2022**, *154*, 106736.
19. Snellings, R.; Reyes, R.A.; Hanein, T.; Irassar, E.F.; Kanavaris, F.; Maier, M.; Marsh, A.T.; Valentini, L.; Zunino, F.; Diaz, A.A. Paper of RILEM TC 282-CCL: Mineralogical characterization methods for clay resources intended for use as supplementary cementitious material. *Mater. Struct.* **2022**, *55*, 149.
20. Avet, F.; Scrivener, K. Simple and Reliable Quantification of Kaolinite in Clay Using an Oven and a Balance. In *Calcined Clays for Sustainable Concrete*; RILEM Bookseries; Springer: Berlin/Heidelberg, Germany, 2020; pp. 147–156.
21. Scrivener, K.; Snellings, R.; Lothenbach, B. *A Practical Guide to Microstructural Analysis of Cementitious Materials*; CRC Press: Boca Raton, FL, USA, 2015.
22. *EN196–1*; Methods of Testing Cement in Part 1: Determination of Strength, European Committee for Standardization. Turkish Standards Institute: Ankara, Turkey, 2006.
23. Nguyen, Q.D.; Afroz, S.; Castel, A. Influence of Calcined Clay Reactivity on the Mechanical Properties and Chloride Diffusion Resistance of Limestone Calcined Clay Cement (LC3) Concrete. *J. Mar. Sci. Eng.* **2020**, *8*, 301.
24. Nguyen, Q.D.; Afroz, S.; Zhang, Y.; Kim, T.; Li, W.; Castel, A. Autogenous and total shrinkage of limestone calcined clay cement (LC3) concretes. *Constr. Build. Mater.* **2022**, *314*, 125720.
25. *ASTM C109/C109M*; Standard Test Method for Compressive Strength of Hydraulic Cement Mortars (Using 2-in. or [50 mm] Cube Specimens. ASTM: West Conshohocken, PA, USA, 2021.
26. *ASTM C1437*; Standard Test Method for Flow of Hydraulic Cement Mortar. ASTM: West Conshohocken, PA, USA, 2020.
27. *ASTM C305-20*; Standard Practice for Mechanical Mixing of Hydraulic Cement Pastes and Mortars of Plastic Consistency. ASTM: West Conshohocken, PA, USA, 2020.
28. *ASTM C348-21*; Standard Test Method for Flexural Strength of Hydraulic-Cement Mortars. ASTM: West Conshohocken, PA, USA, 2021.
29. *ASTM C-1698*; Standard Test Method for Compressive Strength of Hydraulic-Cement Mortars (Using Portions of Prisms Broken in Flexure). ASTM: West Conshohocken, PA, USA, 2018.
30. Wang, S.; Gainey, L.; Mackinnon, I.D.; Allen, C.; Gu, Y.; Xi, Y. Thermal behaviors of clay minerals as key components and additives for fired brick properties: A review. *J. Build. Eng.* **2023**, *66*, 105802.
31. Alujas, A.; Fernández, R.; Quintana, R.; Scrivener, K.L.; Martirena, F. Pozzolanic reactivity of low grade kaolinitic clays: Influence of calcination temperature and impact of calcination products on OPC hydration. *Appl. Clay Sci.* **2015**, *108*, 94–101.
32. Lorentz, B.; Shanahan, N.; Zayed, A. Rheological behavior & modeling of calcined kaolin-Portland cements. *Constr. Build. Mater.* **2021**, *307*, 124761.
33. Avet, F.; Snellings, R.; Diaz, A.A.; Ben Haha, M.; Scrivener, K. Development of a new rapid, relevant and reliable (R3) test method to evaluate the pozzolanic reactivity of calcined kaolinitic clays. *Cem. Concr. Res.* **2016**, *85*, 1–11.
34. Avet, F.; Scrivener, K. Investigation of the calcined kaolinite content on the hydration of Limestone Calcined Clay Cement (LC3). *Cem. Concr. Res.* **2018**, *107*, 124–135.